Yeast
Yeast 2013
Published online in Wiley Online Library
(wileyonlinelibrary.com) **DOI:** 10.1002/yea.2940

Research Article

The *Saccharomyces cerevisiae* enolase-related regions encode proteins that are active enolases

M. J. Kornblatt[1], J. Richard Albert[2], S. Mattie[2], J. Zakaib[2], S. Dayanandan[2,3], P. J. Hanic-Joyce[1] and P. B. M. Joyce[1,3]*

[1]*Department of Chemistry and Biochemistry, Concordia University, Montréal, Canada*
[2]*Department of Biology, Concordia University, Montréal, Canada*
[3]*Centre for Structural and Functional Genomics, Concordia University, Montréal, Canada*

**Correspondence to:*
P. Joyce, Department of Chemistry and Biochemistry, Concordia University, 7141 Sherbrooke St. W., Montreal, QC H4B 1R6, Canada.
E-mail: Paul.Joyce@concordia.ca

Received: 9 October 2012
Accepted: 11 December 2012

Abstract

In addition to two genes (*ENO1* and *ENO2*) known to code for enolase (EC4.2.1.11), the *Saccharomyces cerevisiae* genome contains three enolase-related regions (*ERR1*, *ERR2* and *ERR3*) which could potentially encode proteins with enolase function. Here, we show that products of these genes (Err2p and Err3p) have secondary and quaternary structures similar to those of yeast enolase (Eno1p). In addition, Err2p and Err3p can convert 2-phosphoglycerate to phosphoenolpyruvate, with kinetic parameters similar to those of Eno1p, suggesting that these proteins could function as enolases *in vivo*. To address this possibility, we overexpressed the *ERR2* and *ERR3* genes individually in a double-null yeast strain lacking *ENO1* and *ENO2*, and showed that either *ERR2* or *ERR3* could complement the growth defect in this strain when cells are grown in medium with glucose as the carbon source. Taken together, these data suggest that the ERR genes in *Saccharomyces cerevisiae* encode a protein that could function in glycolysis as enolase. The presence of these enolase-related regions in *Saccharomyces cerevisiae* and their absence in other related yeasts suggests that these genes may play some unique role in *Saccharomyces cerevisiae*. Further experiments will be required to determine whether these functions are related to glycolysis or other cellular processes.

Keywords: ***Saccharomyces cerevisiae*; enolase-related regions**

Introduction

Enolase (EC4.2.1.11) is the enzyme responsible for the conversion of 2-phosphoglycerate to phosphoenolpyruvate during glycolysis and the reverse reaction during gluconeogenesis. In *Saccharomyces cerevisiae*, there are two genes, *ENO1* and *ENO2*, coding for enolase that share 98% amino acid similarity and 95% identity. Since most enolases, including that of yeast, are dimers, three catalytically active enolases, comprised of both homo- and heterodimers of Eno1p (the *ENO1* gene product) and Eno2p (the *ENO2* gene product) are produced by random assortment *in vivo* (McAlister and Holland, 1982).

Although *ENO1* and *ENO2* encode very similar proteins, the expression of these genes is differentially regulated. In commercially grown baker's yeast, cells produce primarily Eno1p (Westhead and McLain, 1964), while in laboratory strains of *Saccharomyces cerevisiae* grown on glucose, Eno2p predominates and, on non-fermentable carbon sources, such as ethanol or glycerol + lactate, there are similar amounts of the two proteins (McAlister and Holland, 1982). This suggests that the *ENO2* gene contains regulatory regions that mediate glucose-dependent induction of gene expression (Cohen *et al*., 1986). Indeed, the 5′ non-coding regions of both *ENO1* and *ENO2* have been well-studied and shown to contain multiple *cis*-acting

regulatory elements (Cohen *et al*., 1987; Uemura *et al*., 1986, 1987). The *ENO1* and *ENO2* genes contain Gcr1p-binding motifs (Huie *et al*., 1992) and Gcr1p is required for maximum transcription of both genes (Holland *et al*., 1990). Either of two upstream activation sites (UASs) can activate transcription independently (Cohen *et al*., 1986, 1987). Binding sites for the transcription factor Rap1p were mapped to UAS1 elements, while different transcription factors, Ebf1p and Abf1p, bound to the UAS2 elements (Brindle *et al*., 1990). The *ENO1* gene also contains an upstream repression sequence (URS) which prevents the glucose-dependent induction mediated by the regulatory elements described above (Cohen *et al*., 1987). However, *ENO1* expression is not repressed in glucose-grown cultures of strains bearing deletions to genes comprising the SNF complex (Choi *et al*., 2008). The *REE1* gene product is required for glucose-repression of *ENO1* and most likely exerts its effect via interaction with Gal83p, a component of the SNF complex (Choi *et al*., 2008). Clearly, the expression of the enolase genes is under complex control in *Saccharomyces cerevisiae*. Despite this difference in the regulation of *ENO1* and *ENO2* in yeast, either gene product can complement the growth defect of an *eno1eno2* double-null strain growing on glucose (Entelis *et al*., 2006).

The situation may be even more complex in mammals where there are three enolase genes, *ENO1*, *ENO2* and *ENO3*, encoding proteins called α-enolase, γ-enolase and β-enolase, respectively. Athough these isozymes have $>80\%$ sequence identity and $>90\%$ sequence similarity, their cognate genes exhibit tissue-specific expression. While β-enolase is found primarily in skeletal and cardiac muscles, γ-enolase is restricted to neurons and the embryonic form, α-enolase, is found in many tissues (Chen and Giblett, 1976; Pearce, *et al*., 1976). These mammalian isozymes also readily associate to produce both homo- and heterodimers (Rider and Taylor, 1974).

In addition to its central role in glycolysis and gluconeogenesis, enolase recently has been implicated in a number of diverse cellular processes ranging from the import of tRNAs into mitochondria (Entelis *et al*., 2006) and the formation of vacuoles (Decker and Wickner, 2006) in yeast, to an association with nuclei, cell membranes and cytoskeletal elements in *Plasmodium* (Pal-Bhowmick *et al*., 2007) to the modulation of signalling pathways (Subramanian and Miller, 2000, Hafner *et al*., 2012) and the regulation of potassium channels (Renigunta *et al*., 2011) in humans. In addition, large amounts of α-enolase are found in the eyes of many organisms (Wistow *et al*., 1988; Cuthbertson *et al*., 1992; Kathiresan *et al*., 2006), where enolase plays a structural rather than enzymatic role (Wistow *et al*., 1988). Interestingly, the products of the conserved *ENO1* and *ENO2* yeast genes appear to play different roles. In cells engineered to express only one of these two genes, both the tRNA import (Entelis *et al*., 2006) and vacuole fusion (Decker and Wickner, 2006) processes function more efficiently with Eno2p than with Eno1p. In humans, *ENO1* also encodes Myc-binding protein-1 (MBP1) which functions in downregulating the activity of the c-myc proto-oncogene (Subramanian and Miller, 2000) and interacts with the renal epithelial K^+ channel ROMK2 to regulate its function (Renigunta *et al*., 2011), while a *C*-terminal peptide of human γ-enolase can mediate neurotrophic effects by activating specific signalling pathways (Hafner *et al*., 2012). It therefore seems that enolase has taken on additional roles throughout a broad spectrum of organisms. Interestingly, in an enolase-depleted yeast strain, *Plasmodium* enolase complements growth retardation, vacuolar fragmentation and altered expression of certain vacuolar proteins (Das *et al*., 2011), suggesting that these additional activities may be evolutionarily conserved. The conservation of accessory functions is also supported by the ability of enolases from diverse organisms to bind plasminogen (reviewed in Kornblatt *et al*., 2011).

Given that enolase plays a role in the central metabolic pathway of glycolysis and gluconeogenesis and functions in diverse processes not linked directly to glycolysis or gluconeogenesis, it is noteworthy that the *Saccharomyces cerevisiae* genome contains, in addition to the well-studied *ENO1* and *ENO2* genes, three additional genes which could encode enolase-like proteins (Pryde *et al*., 1995). These genes were annotated as enolase-related repeats (*ERR1*, *ERR2* and *ERR3*) and are found near the ends of chromosomes XV (YOR393W), XVI (YPL281C) and XIII (YMR323W), respectively. While *ERR1* and *ERR2* have identical open reading frame (ORF) sequences and their predicted gene products have 67% sequence identity with Eno1p and Eno2p, including conservation of all of the amino acids known to be essential for

DOI: 10.1002/yea

the glycolytic and gluconeogenic functions of enolase (Figure 1), the *ERR3* ORF differs from *ERR1* and *ERR2* at 12 nucleotide positions, resulting in only two amino acid differences (glutamate residues at positions 80 and 229 in Err2p are aspartate and lysine residues, respectively, in Err3p). The proximity of the ERR genes to telomeres raises the possibility that transcription of these genes might be reduced, due to the telomere position effect (reviewed in Wellinger and Zakian, 2012) and there is conflicting evidence as to the synthesis and amounts of ERR transcripts or proteins in yeast. While Lipson *et al*. (2009) could detect no transcripts for *ERR3* and reported that transcript levels for *ERR1* and *ERR2* are < 1 transcript/million, suggesting that these genes are likely not transcribed, other data (Ideker *et al*., 2001; Torres *et al*., 2007; Lai *et al*., 2008; Ni *et al*., 2009) suggest that these genes are transcribed and that their expression may be regulated. These different findings may reflect the growth conditions examined. For example, while Lipson *et al*. (2009) analysed transcripts from yeast grown in rich medium with glucose at 30°C, Ideker *et al*. (2001) examined the response to different carbon sources. While null mutations in individual or combinations of ERR genes had no detectable effect on either growth or meiotic viability at room temperature, 30°C or 37°C on fermentable or non-fermentable carbon sources or on sporulation medium, it is possible that functions of these ERR genes may have been compensated for by the *ENO1* and *ENO2* genes, which were still present (Pryde *et al*., 1995). Deutscher *et al*. (2006) proposed that deletions of *ERR2* or *ERR3* would be synthetically lethal with deletions in *ENO1* or *ENO2*, although this has not been tested experimentally. There is evidence that the ERR gene products interact with other proteins in the cell (e.g. Tarassov *et al*., 2008; Costanzo *et al*., 2010) and recently the *ERR2* gene product has been identified as a potential target for protein kinases encoded by *PHO85* (Ptacek *et al*., 2005) and *SCY1* (Fasolo *et al*., 2011), while *ERR1* has been identified as a possible substrate for the kinase encoded by *ELM1* (Sharifpoor *et al*., 2012). Recently, the presence of Err proteins in yeast was reported by Costenoble *et al*. (2011), who noted changes in Err protein levels depending on the carbon source provided (these experiments could not distinguish between Err1p, Err2p and Err3p, given their sequence conservation). In fact, changes in the levels of the Err proteins correlated well with changes in Eno2p levels, as well as with changes in the levels of other glycolytic enzymes (Costenoble *et al*., 2011).

Given these observations, we set out to explore the potential functions of these enolase-related sequences. Here we report that *ERR2* and *ERR3* encode functional enolases, with physical and kinetic properties similar to those of Eno1p. Furthermore, we show that overexpressing either the *ERR2* or *ERR3* gene can complement the growth defect in a double-null yeast strain lacking *ENO1* and *ENO2* when the cells are growing in medium containing glucose as the carbon source. In addition, we found that the Err proteins of *S. cerevisiae* are closely related to Eno1p of *C. glabrata*, whereas both Eno1p and Eno2p of *S. cerevisiae* are closely related to Eno2p of *C. glabrata*.

Materials and methods

Strains and plasmids

Escherichia coli strains XL2 Blue (Stratagene) and BL21(DE3) (Invitrogen) were used for DNA manipulations and protein production, respectively. *Saccharomyces cerevisiae* strain BY4743 (Brachmann *et al*., 1998) was used as a source of genomic DNA for amplification by PCR. The *S. cerevisiae eno2* null strain (relevant genotype *eno2::HIS3 ura3-52 trp1-903*), the enolase-lacking strain (relevant genotype *eno1::kanMX4 eno2::HIS3 ura3 trp1*) designated herein as *eno1eno2* double null and derivatives containing pE1 and pE2 are as described in Entelis *et al*. (2006), and were kindly provided by Dr Nina Entelis (CNRS-Université Louis Pasteur, Strasbourg). *S. cerevisiae* strain W303-1B (R. Rothstein, Columbia University) was used as a control *ENO1 ENO2* strain. Plasmids pET-3a (Novagen) and pG145-3 were used for expression in *E. coli* and yeast, respectively. Plasmid pG145-3 was generated by transferring the *TDH3* promoter, multiple cloning site and CYC terminator of p426GPD (Mumberg *et al*., 1995) into the *Sac*I and *Kpn*I sites of pRS314 (Sikorski and Heiter, 1989).

Plasmid construction

Standard molecular biology techniques were employed throughout (Ausubel *et al*., 1989). Oligonucleotides

DOI: 10.1002/yea

```
YOR393W/Err1p      SITKVHARTVYDSRGNPTVEVEITTENGLFRAIVPSGASTGIHEAVELRDGNKSEWMGKG 60
YPL281C/Err2p      SITKVHARTVYDSRGNPTVEVEITTENGLFRAIVPSGASTGIHEAVELRDGNKSEWMGKG 60
YMR323W/Err3p      SITKVHARTVYDSRGNPTVEVEITTENGLFRAIVPSGASTGIHEAVELRDGNKSEWMGKG 60
YGR254W/Eno1p      AVSKVYARSVYDSRGNPTVEVELTTEKGVFRSIVPSGASTGVHEALEMRDGDKSKWMGKG 60
YHR174W/Eno2p      AVSKVYARSVYDSRGNPTVEVELTTEKGVFRSIVPSGASTGVHEALEMRDEDKSKWMGKG 60
                   :::**:**:*************:***:*:**:*********:***:*:** :**:*****

YOR393W/Err1p      VTKAVSNVNSIIGPALIKSELCVTNQKGIDELMISLDGTSNKSRLGANAILGVSLCVARA 120
YPL281C/Err2p      VTKAVSNVNSIIGPALIKSELCVTNQKGIDELMISLDGTSNKSRLGANAILGVSLCVARA 120
YMR323W/Err3p      VTKAVSNVNSIIGPALIKSDLCVTNQKGIDELMISLDGTSNKSRLGANAILGVSLCVARA 120
YGR254W/Eno1p      VLHAVKNVNDVIAPAFVKANIDVKDQKAVDDFLISLDGTANKSKLGANAILGVSLAASRA 120
YHR174W/Eno2p      VMNAVNNVNNVIAAAFVKANLDVKDQKAVDDFLLSLDGTANKSKLGANAILGVSMAAARA 120
                   * :**.***.:*..*::*::: *.:**.:*::::*****:***:**********:..:**

YOR393W/Err1p      AAAQKGITLYKYIAELADARQDPFVIPVPFFNVLNGGAHAGGSLAMQEFKIAPVGAQSFA 180
YPL281C/Err2p      AAAQKGITLYKYIAELADARQDPFVIPVPFFNVLNGGAHAGGSLAMQEFKIAPVGAQSFA 180
YMR323W/Err3p      AAAQKGITLYKYIAELADARQDPFVIPVPFFNVLNGGAHAGGSLAMQEFKIAPVGAQSFA 180
YGR254W/Eno1p      AAAEKNVPLYKHLADLSKSKTSPYVLPVPFLNVLNGGSHAGGALALQEFMIAPTGAKTFA 180
YHR174W/Eno2p      AAAEKNVPLYQHLADLSKSKTSPYVLPVPFLNVLNGGSHAGGALALQEFMIAPTGAKTFA 180
                   ***:*.:.**:::*:*:.:: .*:*:****:******:****:**:*** ***.**::**

YOR393W/Err1p      EAMRMGSEVYHHLKILAKEQYGPSAGNVGDEGGVAPDIDTAEDALDMIVEAINICGYEGR 240
YPL281C/Err2p      EAMRMGSEVYHHLKILAKEQYGPSAGNVGDEGGVAPDIDTAEDALDMIVEAINICGYEGR 240
YMR323W/Err3p      EAMRMGSEVYHHLKILAKEQYGPSAGNVGDEGGVAPDIDTAEDALDMIVKAINICGYEGR 240
YGR254W/Eno1p      EALRIGSEVYHNLKSLTKKRYGASAGNVGDEGGVAPNIQTAEEALDLIVDAIKAAGHDGK 240
YHR174W/Eno2p      EAMRIGSEVYHNLKSLTKKRYGASAGNVGDEGGVAPNIQTAEEALDLIVDAIKAAGHDGK 240
                   **:*:*:******:** :::**.**************:*:***:***:**.**: .*::*:

YOR393W/Err1p      VKVGIDSAPSVFYKDGKYDLNFKEPNSDPSHWLSPAQLAEYYHSLLKKYPIISLEDPYAE 300
YPL281C/Err2p      VKVGIDSAPSVFYKDGKYDLNFKEPNSDPSHWLSPAQLAEYYHSLLKKYPIISLEDPYAE 300
YMR323W/Err3p      VKVGIDSAPSVFYKDGKYDLNFKEPNSDPSHWLSPAQLAEYYHSLLKKYPIISLEDPYAE 300
YGR254W/Eno1p      IKIGLDCASSEFFKDGKYDLDFKNPNSDKSKWLTGPQLADLYHSLMKRYPIVSIEDPFAE 300
YHR174W/Eno2p      VKIGLDCASSEFFKDGKYDLDFKNPESDKSKWLTGVELADMYHSLMKRYPIVSIEDPFAE 300
                   :*:*:*.*.* *:*******:**:*:** *:**:  :**: ****:*:***:*:***:**

YOR393W/Err1p      DDWSSWSAFLKTVNVQIIADDLTCTNKTRIARAIEEKCANTLLLKLNQIGTLTESIEAAN 360
YPL281C/Err2p      DDWSSWSAFLKTVNVQIIADDLTCTNKTRIARAIEEKCANTLLLKLNQIGTLTESIEAAN 360
YMR323W/Err3p      DDWSSWSAFLKTVNVQIIADDLTCTNKTRIARAIEEKCANTLLLKLNQIGTLTESIEAAN 360
YGR254W/Eno1p      DDWEAWSHFFKTAGIQIVADDLTVTNPKRIATAIEKKAADALLLKVNQIGTLSESIKAAQ 360
YHR174W/Eno2p      DDWEAWSHFFKTAGIQIVADDLTVTNPARIATAIEKKAADALLLKVNQIGTLSESIKAAQ 360
                   ***.:** *:**..:**:***** **  *** ***:*.*::****:******:***:**:

YOR393W/Err1p      QAFDAGWGVMISHRSGETEDPFIADLVVGLRCGQIKSGALSRSERLAKYNELLRIEEELG 420
YPL281C/Err2p      QAFDAGWGVMISHRSGETEDPFIADLVVGLRCGQIKSGALSRSERLAKYNELLRIEEELG 420
YMR323W/Err3p      QAFDAGWGVMISHRSGETEDPFIADLVVGLRCGQIKSGALSRSERLAKYNELLRIEEELG 420
YGR254W/Eno1p      DSFAAGWGVMVSHRSGETEDTFIADLVVGLRTGQIKTGAPARSERLAKLNQLLRIEEELG 420
YHR174W/Eno2p      DSFAANWGVMVSHRSGETEDTFIADLVVGLRTGQIKTGAPARSERLAKLNQLLRIEEELG 420
                   ::* *.****:*********.********** ****:** :******* *:*********

YOR393W/Err1p      DDCIYAGHRFHDGNKL 436
YPL281C/Err2p      DDCIYAGHRFHDGNKL 436
YMR323W/Err3p      DDCIYAGHRFHDGNKL 436
YGR254W/Eno1p      DNAVFAGENFHHGDKL 436
YHR174W/Eno2p      DKAVYAGENFHHGDKL 436
                   *..::**..**.*:**
```

Figure 1. ClustalW alignment of yeast enolases and the predicted products from the enolase-related regions of the yeast genome. The numbering used in the alignment is based on the initial sequencing of Eno1p (Chin *et al*., 1981), from which the *N*-terminal methionine had been removed. Residues identified to be involved in mechanism by mutagenesis and crystal structure (Larsen *et al*., 1996) and residues that bind the first metal ion (Wedekind *et al*., 1995) are shown in bold. Residues involved in hydrogen bonds or salt links between subunits (Stec and Lebioda, 1990) are shown in bold and italic. Additional residues predicted by computational studies to be involved in the mechanism (Liu *et al*., 2000) are shown in italic. The three highly mobile loops (Stec and Lebioda, 1990; Wedekind, *et al*., 1994) are underlined. (*), amino acid identity; (:), strongly conserved amino acids; (.) weakly conserved amino acids

DOI: 10.1002/yea

used in plasmid construction are listed in Table 1. The enolase-related ORFs were cloned in two segments. The 3′ portion of the ORFs was obtained by PCR amplification of 1.3 kbp regions from BY4743 genomic DNA, using oligonucleotides ERR2a and ERR2b. This PCR reaction simultaneously amplified *ERR3*, *ERR1* and *ERR2* sequences from chromosomes XIII, XV and XVI, respectively. The resulting products were digested with *Nde*I and *Bam*HI and the 600 bp *Nde*I/*Bam*HI fragment population was ligated into similarly-digested pET-3a. The five nucleotide differences between *ERR3* and both *ERR1* or *ERR2* (which are identical) in this region are silent, and therefore the same cloned representative *Bam*HI/*Nde*I fragment was used to construct both the *ERR2* and *ERR3* clones. An *Nde*I/*Nde*I fragment from the same digest was used to clone the 5′ end of the open reading frame and this region contains seven nucleotide differences defining two amino acid substitutions that are diagnostic of *ERR2* or *ERR3*. This *Nde*I/*Nde*I fragment was ligated into the pET-3a vector-derivative upstream of the inserted *Nde*I/*Bam*HI fragment, and DNA sequence analysis was used to distinguish between *ERR2* and *ERR3* sequences (as *ERR1* and *ERR2* are identical from at least 500 bp upstream to 300 bp downstream of their open reading frames, we chose to name the clone *ERR2* and used it as a representative of both genes). For expression in *S. cerevisiae*, the *ERR2* and *ERR3* clones were amplified independently from the appropriate pET-3a derivatives by PCR, using the ERRBAM5′ and ERRSAL3 primers, digested with *Bam*HI and *Sal*I and ligated into *Bam*HI/*Sal*I-digested pG145-3. The *ENO1*and *ENO2* genes were amplified by PCR from BY4743 genomic DNA, using the ENO5BAM and ENO1-3SAL or ENO2-3SAL oligonucleotides, respectively, digested with *Bam*HI and *Sal*I and ligated to similarly-digested pG145-3. Oligonucleotides were purchased from Biocorp (Montreal, QC, Canada). All plasmid constructs were confirmed by sequence analysis (McGill University and Génome Québec Innovation Centre, Canada).

Plasmid shuffling

Yeast strain *eno1eno2* + pE2 or the control strain W303-1B was transformed with pG145-3 or derivatives containing the open reading frame of *ERR2*, *ERR3*, *ENO1* or *ENO2* under the control of the *TDH3* promoter. Transformants were selected on synthetic complete medium (Sherman, 1991) lacking uracil and tryptophan. Plasmid shuffling was accomplished by replica-plating Ura^+Trp^+ transformants onto YPD, incubating overnight at room temperature, replica-plating to 5-fluoro-orotic acid (FOA) medium (Boeke *et al*., 1984) supplemented with 30 mg/l leucine, lysine and tyrosine and 20 mg/l adenine, histidine and tryptophan, with or without FOA, and incubating at 30°C for 4 days.

Growth assays

FOA-resistant transformants were grown overnight at 30°C in SC–trp medium (except for the *eno1eno2* or the *eno1eno2* + pE2 strains, which were grown for 1 week on YPG plates (Sherman, 1991) or in SC liquid medium lacking uracil, respectively). The cells were diluted in phosphate-buffered saline (PBS) to a concentration of 0.5 OD_{600} units, serially diluted, spotted onto the appropriate medium and incubated at 30°C for the times indicated.

Table 1. Oligonucleotides used in this study

Oligonucleotide	Sequence (5′ to 3′)*
ERR2a	GATAAACATATGTCCATCACGAAGGTAC
ERR2b	ACAAGAGGATCCTTTATAGTTTGTTTCCATC
ENO5BAM	GAATTCGGATCCAATGGCTGTCTCTAAAG
ENO1-3SAL	GGTTATGTCGACGTTTTTTGGACTAGAAGGC
ENO2-3SAL	GGTTATGTCGACGAAAAGACTAATAATTCTTAG
ERRBAM5′	GAGGATCCTATGTCCATCACGAAGG
ERRSAL3′	ACAAGGTCGACCTTTATAGTTTGTTTCC

*Restriction sites used are underlined.

DOI: 10.1002/yea

Protein purification

The expression and purification of Eno1p was done following the procedure of Zhao *et al.* (2008). The expression of *ERR2* and *ERR3* was performed as described previously for *ENO1* (Poyner *et al.*, 1996), except that the overnight expression was performed at 29°C. Resuspension of the cells, sonication and ammonium sulphate precipitation have been described previously (Zhao *et al.*, 2008). The precipitated protein was dialysed against TME buffer (50 mM Tris–HCl, pH 7.4, 1 mM $Mg(OAc)_2$ and 0.1 mM EDTA) and applied to a Q-Sepharose column that had been equilibrated with the same buffer. Unbound protein was removed by washing with TME and Err2p or Err3p was eluted with a 0–0.6 M gradient of NaCl in TME. Fractions containing enolase activity were pooled, dialysed overnight against TME and precipitated with 85% ammonium sulphate. The precipitated protein was stored at 4°C and dialysed against TME prior to use. Protein concentrations were determined at 280 nm, using the following extinction coefficient for Err2p and Err3p: 48360 M/cm or 1.025 mg/ml. For crude extracts, the BIORAD protein assay was used with BSA as a standard.

Activity assays

Enzyme activity was measured in a continuous assay by following, at 240 nm, the conversion of 2-phosphoglycerate (PGA) to phosphoenolpyruvate (PEP; $\varepsilon_{PEP} = 1.33\ mM^{-1}$). The assay used during purification contained 50 mM imidazole, pH 7.1, 250 mM KCl, 1 mM $Mg(OAc)_2$, 0.1 mM EDTA and 1 mM PGA. Specific activities (U/mg protein) in crude extracts were determined using this assay. The PGA was prepared enzymatically from ATP and glyceric acid (Sims and Reed, 2005). For kinetic studies, the buffer contained 25 mM Tris and 25 mM 2-(*N*-morpholino)ethanesulphonic acid (MES), pH 7.1. Assays contained either 1 mM PGA and variable concentrations of $Mg(OAc)_2$ in the range 10 μM to 9 mM or 0.5 mM $Mg(OAc)_2$, and variable concentrations of PGA in the range 30–990 μM. Kinetic parameters were determined via non-linear curve fitting with ENZFITTER (Biosoft), using either the Michaelis–Menten equation (for rate vs [PGA]) or the equation for modified substrate inhibition (for rate vs $[Mg^{2+}]$; Kornblatt, 2005); K_{cat} is expressed as U/monomer enzyme. All assays were performed in duplicate from a single purified protein preparation for each enzyme. This ensured consistency between the enzyme assays and all subsequent biophysical characterizations.

Biophysical characterization

Molecular masses were determined by MS-Q-TOF at the Concordia Centre for Biological Applications of Mass Spectrometry. CD spectra were recorded on a Jasco J-810 spectropolarimeter. Samples were 14 μM in TME titrated with H_2SO_4. Spectra were scanned in the range 260–185 nm, using a 0.01 cm path length at 20°C. Subtraction of the buffer spectrum and smoothing of the spectra were done using Jasco software. The resulting spectra were analysed for secondary structure at the Dichroweb site (Birkbeck College, UK) using the CDSSTR method. For temperature denaturation, a 1 mm cuvette was used and the CD signal was monitored at 222 nm, while the temperature was increased from 35°C to 70°C at 15°C/h.

Sedimentation velocity experiments were performed in a Beckman XL-I analytical ultracentrifuge. Samples were 14 μM in TME buffer; centrifugation was at 35 000 rpm at 20°C, with scanning at 280 nm. Data were analysed using SEDFIT v 89 (www.analyticalultracentrifugation.com), using the continuous c(s) model. The viscosity and density for the buffer were calculated using SEDNTERP v 1.07 (D. B. Hayes, T. Laue and J. Philo: www.bbri.org/RASMB/rasmb.html) and used to convert sedimentation coefficients to $s_{20,w}$.

The K_d value for subunit dissociation of the enolases was determined by incubating the enzyme in TME buffer containing varying concentrations of $NaClO_4$. After an incubation of 24 h at 15°C, aliquots were assayed for enzymatic activity using our standard enolase assay. The experiment was performed twice, with each sample being assayed in duplicate. Based on previous experiments (Zhao *et al.*, 2008), we assumed that the fraction of activity, compared to the control in the absence of $NaClO_4$, equals the fraction of dimeric enzyme. These data were then used to calculate K_d:

$$K_d = 4\,[\text{enolase}]\,(f_M)^2/(f_D)$$

where f_M and f_D are the fractions of monomeric and dimeric enzyme, respectively. A plot of log K_d vs $[NaClO_4]$ gives K_d at 0 M $NaClO_4$.

DOI: 10.1002/yea

Phylogenetic analyses

The amino acid sequences of selected enolase gene products were aligned using the ClustalW software program (Thompson *et al*., 1994: www.ebi.ac.uk/Tools/msa/clustalw2) and analysed using PAUP* v 4.0 (Swofford, 2001). Phylogenetic trees were reconstructed through three algorithms: (a) unweighted pair group method with arithmetic mean (UPGMA); (b) neighbour joining (NJ); and (c) maximum parsimony (MP), as implemented in PAUP. The robustness of resulting tree branches was assessed via bootstrap analyses of 1000 replicates.

Results

The release of the complete sequence of the *S. cerevisiae* genome (Goffeau *et al*., 1996) revealed three enolase-related regions, *ERR1*, *ERR2* and *ERR3*, in addition to the two known enolase genes, *ENO1* and *ENO2*. The predicted amino acid sequences of these three enolase-related regions show 99–100% identity with each other and approximately 67% identity with Eno1p and Eno2p. When similar amino acids are taken into account, the ERR sequences are approximately 86% similar to the enolase proteins, and all of the amino acids crucial for enolase enzyme activity are conserved (Figure 1), suggesting that these ERR gene products have retained enolase enzymatic activity.

To test for this, we expressed the *ERR2* and *ERR3* genes in *E. coli* and purified Err2p and Err3p to at least 95% purity, as judged by SDS–PAGE (data not shown), with yields of 40–50 mg/l culture. Since *ERR1* and *ERR2* encode identical proteins, we did not include *ERR1* in our studies. We then compared the physical and kinetic properties of both proteins to those of similarly prepared recombinant yeast Eno1p (Table 2). Eno1p was chosen for the comparison since it is the better-characterized yeast enolase. All three proteins have the expected molecular mass (Table 2), identical secondary structure, as determined by circular dichroism (Table 2, Figure 2), and the same quaternary structure, as judged by AUC sedimentation velocity experiments (Figure 3). The variability in percent α-helix between the three proteins is within the range that we have observed with multiple measurements on a single protein. When compared to Eno1p, Err2p and Err3p are 4–5°C more stable towards temperature denaturation (Table 2). In experiments using sodium perchlorate to dissociate active enolase into inactive monomers (Zhao *et al*., 2008), both ERR proteins were more stable ($K_d = 1–5 \times 10^{-9}$) than Eno1p ($K_d = 71.4 \times 10^{-9}$).

All three enzymes followed Michaelis–Menten kinetics for increasing 2-phosphoglycerate (PGA) concentrations and the K_m and K_{cat} values determined under these conditions for all three enzymes differ by less than four-fold (Table 2). As has been shown previously for Eno1p (Faller *et al*., 1977),

Table 2. Physical and kinetic properties of yeast enolase 1 (Eno1p) and enolase-repeat region gene products (Err2p, Err3p)

Property	Eno1p	Err2p	Err3p
Mass, theoretical	46672	47196	47181
Mass by ESI–MS	46673	47198	47184
Secondary structure			
% Helix	41	45	43
% Sheet	15	15	17
T_m	55.5	60.5	60
K_{cat}, s^{-1}*	71.4 ± 0.5	19.7 ± 0.2	19.4 ± 0.3
K_m (PGA), μM*	32.05 ± 0.89	44.82 ± 1.5	58.56 ± 2.95
K_m (Mg^{2+}), μM**	49.3 ± 4.8	66.6 ± 9.4	65.3 ± 7.3
K_i (Mg^{2+}), mM**	2.1 ± 1	0.327 ± 0.074	0.695 ± 0.20

*K_{cat} and K_m (PGA) determined from *v* vs [PGA], at 0.5 mM Mg^{2+}; value of K_{cat} is calculated in terms of active sites, i.e. the concentration of monomers in the assays.
**Kinetic constants for Mg^{2+} determined from *v* vs [Mg^{2+}] at 1 mM PGA.

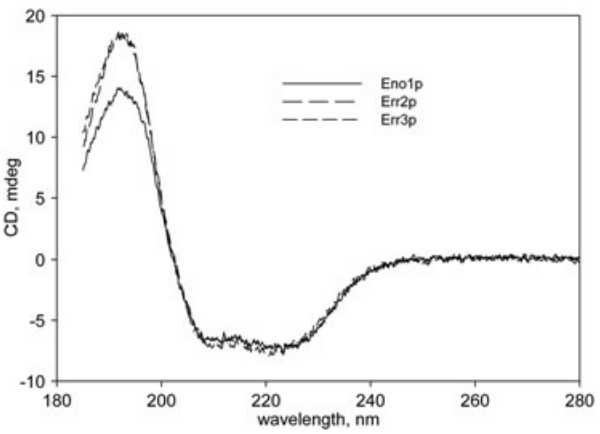

Figure 2. CD spectra of the three proteins. Each protein was suspended at a concentration of 14 μM in TME-SO_4 buffer; spectra were recorded and the data treated as described in Materials and methods

DOI: 10.1002/yea

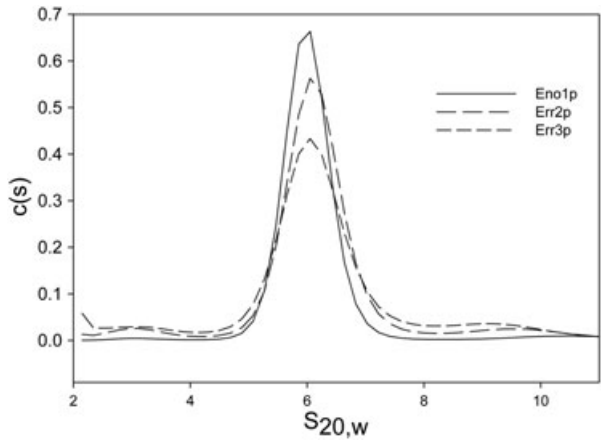

Figure 3. Sedimentation velocity data for the comparison of quaternary structure. Sample preparation, centrifugation and data analysis were performed as described in Materials and methods

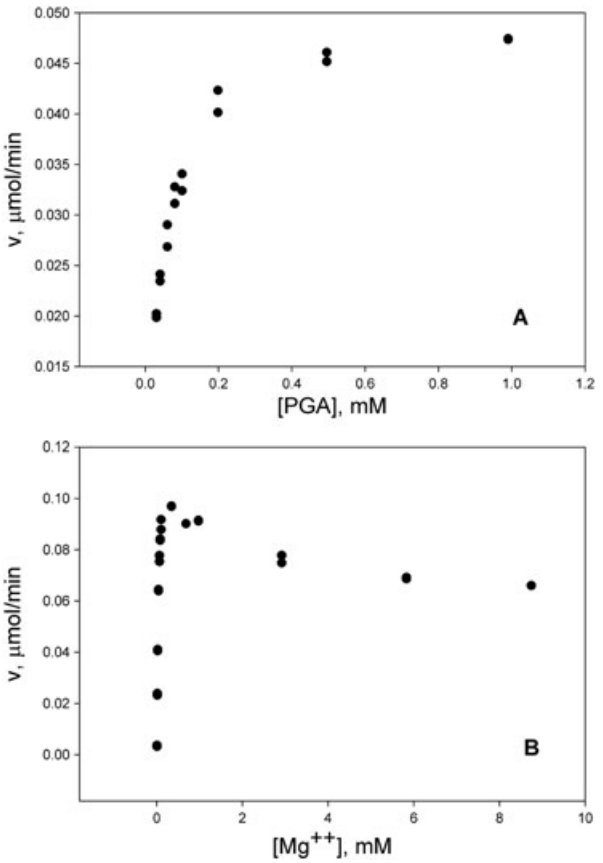

Figure 4. Kinetic data for Err2p. (A) Rate was measured as a function of [PGA], with $[Mg^{2+}]$ constant at 0.5 mM; [Err2p] = 4.2×10^{-8} M. Data were fitted to the Michaelis–Menten equation (see Materials and methods) and the calculated K_m for PGA and K_{cat} are reported in Table 2. (B) Rate was measured as a function of $[Mg^{+2}]$, with PGA constant at 1 mM; [Err2p] = 8.5×10^{-8} M. Data were fitted to the equation for modified substrate inhibition (see Materials and methods) and the K_m and K_i for Mg^{2+} are reported in Table 2

all three enzymes were activated by low concentrations of Mg^{2+} and then inhibited at higher concentrations of Mg^{2+}. To illustrate the effect of increasing Mg^{2+} concentration on enzyme activity, the kinetic data for Err2p are shown (Figure 4). Similar observations were made with the other two enzymes (data not shown). Relative to Eno1p, both Err proteins have higher K_m and K_i values for Mg^{2+}. Taken together, the circular dichroism, analytical ultracentrifuge, temperature denaturation, sodium perchlorate dissociation and enzyme kinetics data indicate that *ERR2* and *ERR3* code for proteins that are similar to yeast Eno1p in both physical and kinetic properties.

To test whether proteins produced from the ERR genes could function *in vivo*, we performed plasmid shuffling into an *eno1eno2* double-null strain bearing a plasmid-borne copy of the *ENO2* gene (*eno1eno2* + pE2). When this double-null strain was co-transformed with the *TRP1*-bearing plasmid pG145-3 or derivatives of this plasmid containing *ERR2*, *ERR3*, *ENO1* or *ENO2* controlled by the glyceraldehyde-3-phosphate dehydrogenase (*TDH3*) promoter, grown on YPD and then replica-plated to medium with or without FOA, the strain bearing empty pG145-3 vector was unable to grow in the presence of FOA (Figure 5), indicating that the *eno1eno2* double-null strain is not viable in glucose-containing medium. In contrast, cells containing pG145-3 derivatives bearing *ENO1*, *ENO2*, *ERR2* or *ERR3* were able to grow on FOA medium, indicating that the Err proteins complemented the growth defect of the double-null strain. We compared growth rates of the *eno1eno2* double-null strain transformed with plasmids carrying *ENO1*, *ENO2*, *ERR2* or *ERR3* expressed from the *TDH3* promoter to cells expressing *ENO1* or *ENO2* under the control of their own promoters on glucose or galactose media (Figure 5). As reported by Entelis *et al.* (2006), the growth defect of the *eno1eno2* double-null strain on YPD medium was complemented by either *ENO1* (+pE1) or *ENO2* (+pE2) under the control of its own promoter on a low copy number plasmid (Figure 5). Cells expressing either *ERR2* or *ERR3* from the *TDH3* promoter grew more slowly

DOI: 10.1002/yea

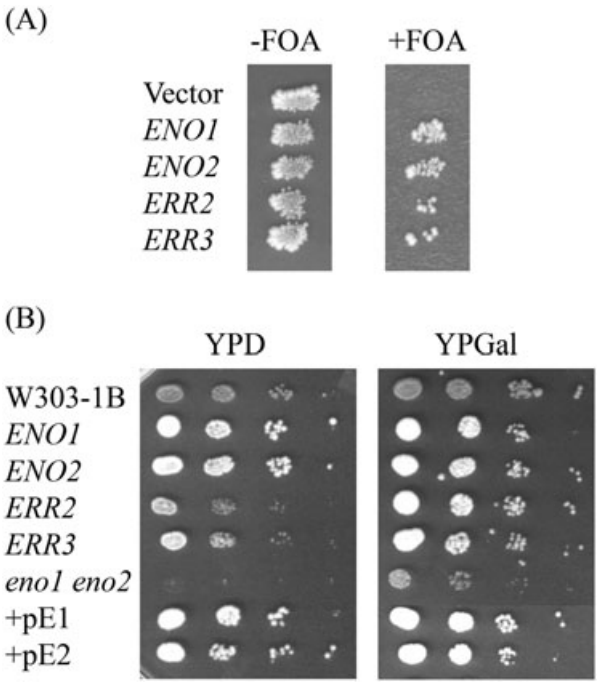

Figure 5. Growth characteristics of transformants bearing plasmid-borne enolase and enolase-related genes. (A) Plasmid shuffling by 5-FOA selection. An *eno1eno2* double-null strain bearing a plasmid containing *ENO1* and *URA3* genes was transformed with a second plasmid bearing only the *TRP1* gene (vector) or the *TRP1* gene and enolase (*ENO1*, *ENO2*) or enolase-related genes (*ERR2*, *ERR3*) expressed from the *TDH3* promoter. The ability of two independent transformants to grow on synthetic medium, with or without 5-FOA, was assessed by replica-plating and incubation at 30 °C for 4 days. (B) Comparison of growth rates on different carbon sources. An *eno1eno2* double-null strain containing plasmid-borne enolase or enolase-related genes expressed from the *TDH3* promoter (*ENO1*, *ENO2*, *ERR2*, *ERR3*) or from their native promoters (*ENO1* or *ENO2*, designated + pE1 and + pE2, respectively) was grown to logarithmic phase in SC-trp medium. Equivalent numbers of cells were diluted serially, spotted on medium containing either glucose (YPD) or galactose (YPG) and incubated at 30 °C for 2 or 3 days, respectively. Cells expressing both wild-type chromosomal *ENO1* and *ENO2* genes and bearing the *TRP1*-containing vector alone (W303-1B) and recipient cells lacking plasmids (*eno1eno2*) were also diluted and spotted

than cells expressing *ENO1* or *ENO2* from either the native or *TDH3* promoter. This latter observation was supported by growth curves for the same cells from liquid cultures with glucose as the carbon source (2–2.5 h doubling times were observed for cells expressing *ENO1* or *ENO2*, while 3–3.5 h doubling times were observed for cells expressing *ERR2* and *ERR3*, respectively). Again in good agreement with what had been reported by Entelis *et al*. (2006), the *eno1eno2* double-null strain was able to grow using galactose as a carbon source (Figure 5). Moreover, all cells carrying plasmid-borne enolase or enolase-related genes showed growth on galactose medium (Figure 5).

When plasmids containing *ENO1*, *ERR2* or *ERR3* under the control of the glyceraldehyde-3-phosphate dehydrogenase promoter (*TDH3*) were expressed in a yeast strain lacking both *ENO1* and *ENO2*, the specific activities of the crude extracts of *ERR2*- or *ERR3*-carrying cells were 24% and 31%, respectively, of the values obtained for the strain carrying *ENO1*. This is in good agreement with the data for the purified proteins (K_{cat} of Err2p or Err3p is about 30% that of Eno1p; Table 2) and suggests that the concentration of Err2p or Err3p or Eno1p is similar in these overexpressing strains. The most straightforward explanation for this is that all proteins are expressed equally well from the *TDH3* promoter and that Err2p, Err3p and Eno1p have similar stabilities in the cell. The specific activity of enolase (1.14 μM/min/mg protein) in a crude extract from an *eno2*-null strain carrying only the chromosomal copy of the *ENO1* gene was similar to that of the strains overexpressing *ERR2* (1.02 μM/min/mg protein) or *ERR3* (1.58 μM/min/mg protein), indicating that the overexpression of *ERR2* or *ERR3* compensates for the reduced specific activity of Err2p or Err3p, such that all of these cells have the same amount of 'enolase activity' for glycolysis and gluconeogenesis.

To assess whether other yeasts contain these enolase-related type genes, we searched the completed yeast genome sequences accessible through the Génolevures genome browser (http://www.genolevures.org/yeastgenomes.html) for enolase-encoding sequences. None of the other yeast species have as many enolase-type genes as *S. cerevisiae*. *Debaryomyces hansenii* had the next largest number of enolase-type sequences, two encoding complete ORFs and another containing a truncated ORF. *Candida glabrata* and *Pichia sorbitophila* both contained two enolase-type genes, while *Zygosaccharomyces rouxii*, *Kluyveromyces thermotolerans*, *S. kluyveri*, *Ashbya gossypii* and *Yarrowia lipolytica* each contained a single enolase-type gene. All three methods of phylogenetic analyses employed resulted in similar phylogenetic tree topologies with the exception of the relative positions of *A. gossypii* Eno1p, *S. kluyveri* Eno1p and *D. hansenii* Eno1p, which varied among trees

DOI: 10.1002/yea

(see Supporting information, Figure S1). The relatedness among these gene products is shown in a distance-based UPGMA tree (Figure 6), and the pairwise distances are given in Table S1 (see Supporting information). With the exception of the *Z. rouxii* and *K. thermotolerans* proteins, the protein sequences clustered into four major groups. One group comprised Eno1p of *A. gossypii*, *K. lactis* and *S. kluyveri*, while another closely related group comprised Eno2p of *C. glabrata* and Eno1p and Eno2p of *S. cerevisiae*. The third group consisted of Eno2p of *D. hansenii* and EnoEp and EnoFp of *P. sorbitophila*, while the fourth group consisted of Eno1p of *D. hansenii*, *Y. lipolytica* and *C. glabrata* and Err2p and Err3p of *S. cerevisiae*. *Saccharomyces* Eno1p and Eno2p clustered tightly but separately from the also tightly-clustered Err2p and Err3p. The resulting phylogenetic tree topologies and high bootstrap values (> 95%) strongly suggest that the closest relative of *S. cerevisiae* Err2p and Err3p is Eno1p of *C. glabrata*, whereas Eno1p and Eno2p of *S. cerevisiae* are closely related to Eno2p of *C. glabrata*.

Discussion

Enolase is a key enzyme catalysing one of the steps in the conserved central metabolic pathways of glycolysis and gluconeogenesis. In *Saccharomyces cerevisiae* there are two genes that code for enolases and both have been shown to catalyse the reversible interconversion of 2-phosphoglycerate to phosphoenolpyruvate. In addition, three enolase-related regions have been identified in the *Saccharomyces cerevisiae* genome, which could potentially encode functional enolases. In fact, of all of the amino acids

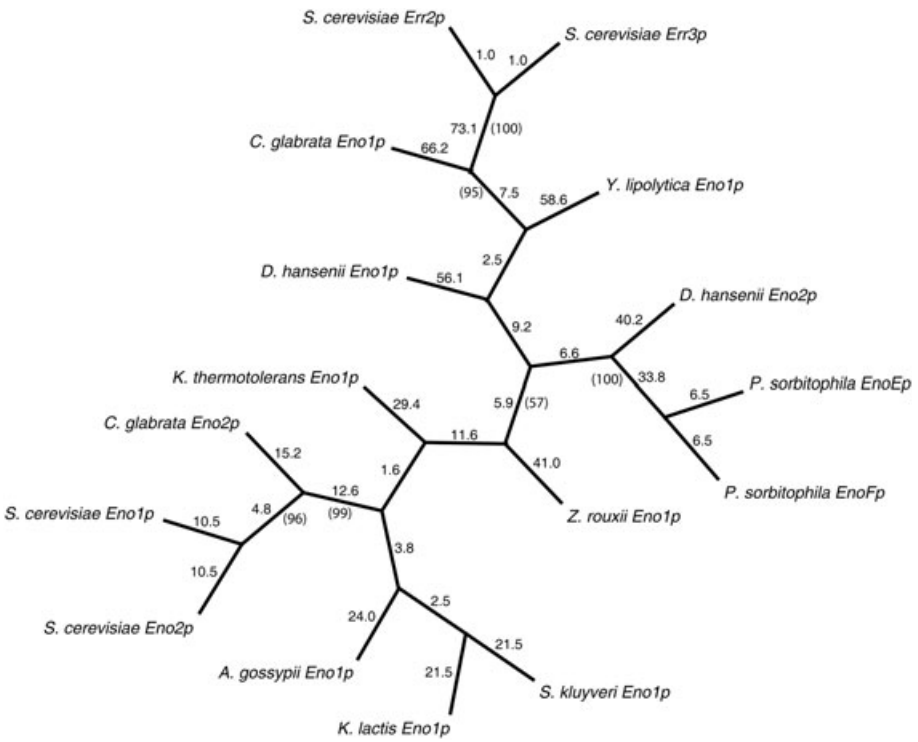

Figure 6. The unrooted, unweighted pair-group method with arithmetic mean (UPGMA) phylogenetic tree, based on pairwise distances of amino acid sequences of enolase and enolase-related gene products from *Saccharomyces cerevisiae*, *Debaryomyces hansenii*, *Candida glabrata*, *Pichia sorbitophila*, *Zygosaccharomyces rouxii*, *Kluyveromyces thermotolerans*, *Saccharomyces kluyveri*, *Ashbya gossypii* and *Yarrowia lipolytica*. If the gene coding for the protein had been annotated, the available annotation was used. If an organism had a single sequence similar to enolase that had not been annotated as an enolase, it was arbitrarily coded as Eno1p. In *Pichia sorbitophila*, where two genes are present, the coding indicates the chromosome (E or F) on which the gene was found. The numbers within brackets indicate the bootstrap values (> 50%), based on parsimony analyses of 1000 replicates

DOI: 10.1002/yea

that have been identified as important for enolase enzyme activity by mutagenesis, crystallography or computational analysis, there is only one residue, glutamate 251, that is not conserved (Figure 1). This residue has been implicated in the mechanism based on computational analysis (Liu *et al*., 2000), and is represented by valine in Err2p and Err3p. The amino acids that are conserved include those that bind the substrate and both molecules of the required divalent cation (Larsen *et al*., 1996; Wedekind *et al*., 1995; Zhang *et al*., 1994), those directly implicated in catalysis (Poyner *et al*., 1996) and those proposed, on the basis of computational analysis (Liu *et al*., 2000), to stabilize one or the other of the two transition states. In addition, residues that have been described as forming salt links or hydrogen bonds between the two subunits (Stec and Lebioda, 1990) are also completely conserved. Given this level of conservation at the amino acid level, including those amino acids involved both in structure and function, we expected that Err2p and Err3p would show characteristics of enolases. This expectation was proven correct for all parameters investigated. The molecular masses of all three proteins were as predicted (Table 2) and the secondary structures of all three proteins, as determined by circular dichroism, were the same. All three proteins showed about 15% β-sheet and about 43% α-helical character (Table 2). This is in good agreement with the known crystal structure of Eno1p (Stec and Lebioda, 1990) and the characteristics of other known enolases (Kang *et al*., 2008; Chai *et al*., 2004; Kűhnel and Luisi, 2001; Duquerroy *et al*., 1995; da Silva Giotto *et al*., 2003). Moreover, Err2p and Err3p have dimeric quaternary structure, as determined by analytical ultracentrifugation (Figure 3). Eno1p, which is known to exist primarily as a dimer (Brewer and Weber, 1968), has a sedimentation coefficient of 6.01, while Err2p and Err3p have sedimentation coefficients of 6.15 and 6.16, respectively, indicating that they are dimeric. For each protein, the dimeric species accounts for 80–86% of the total protein, while smaller amounts of monomer ($s_{20,w}$ of ~3) and trace amounts of larger oligomeric forms also are present. Taken together, these data demonstrate that Err2p and Err3p fold with secondary structures characteristic of Eno1p and assume the typical dimeric quaternary structure of native yeast enolase (Eno1p). The only difference in physical properties that we have observed is that Err2p and Err3p show, relative to Eno1p, an increased temperature stability and resistance to dissociation by sodium perchlorate. Column chromatographic separation of the recombinant proteins showed that Err2p or Err3p eluted at a salt concentration similar to that reported (McAlister and Holland, 1982) for elution of Eno2p. This co-elution profile may explain why the Err proteins were not detected previously.

Given that Err2p and Err3p show a higher order structure similar to Eno1p and possess all of the amino acids shown to be required for enzyme activity, it was not surprising that the kinetic behaviours of Err2p and Err3p were similar to that of Eno1p (Table 2). All three enzymes catalyse the conversion of PGA into PEP with similar kinetic constants, including the values of K_{cat}. The small differences in kinetic values likely reflect subtle differences at the active site. A comparison of the X-ray structures of Eno1p, with and without substrates or analogues bound (Zhang *et al*., 1994; Wedekind *et al*., 1994), revealed the existence of three mobile loops that change position upon binding of substrate and Mg^{2+}. Loops 1 (amino acids 37–41 in the Eno1p sequence, underlined in Figure 1) and 2 (amino acids 155–165 in the Eno1p sequence, underlined in Figure 1), which have been implicated in the mechanism, are completely conserved in their primary sequence between Err2p, Err3p and Eno1p. The third loop (amino acids 247–284 in Eno1p, underlined in Figure 1), which moves with the first two, perhaps to maintain van der Waals contacts in the core of the protein (Wedekind *et al*., 1994), shows six, non-conserved substitutions in Err2p and Err3p, including the introduction of three prolines. It will be interesting to explore whether these changes in the sequence of loop three are involved in the altered kinetic properties of Err2p and Err3p, as compared to Eno1p.

The amino acids of the subunit interface in Eno1p are conserved in Err2p and Err3p, except for two positions; alanine at position 203 of Eno1p is proline in Err2p and Err3p, and proline at position 400 of Eno1p is leucine in the Err proteins. While residue 203 is at the edge of the interface and may not contribute significantly to the subunit interactions, proline 400 is on a loop that contains two residues, 402 and 403, that make hydrogen bonds with the other subunit. Changing a proline to leucine could change the conformation of this loop and might account for the stronger subunit interactions, as reflected in the K_d values.

DOI: 10.1002/yea

Overall, the majority of amino acids required to define the structure and function of enolase have been retained in Err2p and Err3p and, as a result of this, the Err2p and Err3p proteins show structural and enzymatic characteristics typical of enolases. Moreover, the ERR genes complemented the growth defect in *eno1eno2* double-null cells grown on glucose (Figure 5), suggesting that all or some of the functions of Eno1p and Eno2p can be replaced by Err2p or Err3p. The specific activity of enolase in crude extracts of strains carrying the plasmids overexpressing *ERR2* or *ERR3* was similar to that of cells expressing only the chromosomal copy of *ENO1*; however, the cells bearing the ERR genes grew less well. This may suggest that these enzymes are not carrying out the glycolytic/gluconeogenic reaction as efficiently as the native enzyme *in vivo*, or perhaps that there are other activities of enolase, in addition to glycolysis and gluconeogenesis, that these enzymes cannot perform. The fact that these ERR genes actually do function in glycolysis in *Saccharomyces cerevisiae* may help to explain the observation that the *eno1eno2* double-null strain (Entelis *et al*., 2006) can grow using galactose (Figure 5). This may be the result of the complex regulation of the enzymes of central metabolism and differences in that regulation that depend on the carbon source being used. A classic example of this is the Crabtree effect, i.e. the occurrence of alcoholic fermentation under aerobic conditions when glucose is abundant. In this case the pyruvate produced via glycolysis is channelled into ethanol production, rather than to acetyl-CoA and the tricarboxylic acid (TCA) cycle. One possible explanation for our observations is that the *eno1eno2* double-null cells express low levels of enolase from the *ERR* genes. In the context of the repression of the ERR genes (Lipson *et al*., 2009) and the reduction in TCA cycle enzymes (Costenoble *et al*., 2011) when cells are grown on glucose as compared to galactose, the level of enolase activity is not sufficient to support growth of the *eno1eno2* double-null strain, as most ATP is produced via glycolysis. In contrast, on galactose sufficient ATP is being produced via glycolysis and the TCA cycle to support growth.

The presence of multiple ENO and ERR genes in *Saccharomyces cerevisiae* could be attributable to a whole-genome duplication and/or gene duplication events. Wolfe and Shields (1997) suggest that *Saccharomyces cerevisiae* ENO genes are the result of a genome duplication event. The clustering of Eno1p and Eno2p of *S. cerevisiae* with *C. glabrata* Eno2p in a group distinct from the cluster which comprises Eno1p of *C. glabrata*, and Err2p and Err3p of *S. cerevisiae*, suggests that these two groups may have diverged after the initial genome duplication that is common to both of these yeasts (Dujon *et al*., 2004). Furthermore, the close amino acid sequence similarity between Eno1p and Eno2p, and also between *ERR1*, *ERR2* and *ERR3* of *S. cerevisiae*, suggests that these genes may have originated through gene duplication events following the genome duplication. Thus, we suggest that an initial ENO gene was duplicated through the original genome duplication and further duplicated and diverged, giving rise to multiple, closely-related ENO and ERR genes. We suggest that the highly similar *ENO1* and *ENO2* genes in *S. cerevisiae* arose from a gene duplication event in *S. cerevisiae* after the divergence of *S. cerevisiae* and *C. glabrata*. Moreover, after the original ERR gene had diverged from the ENO gene, it underwent at least two duplications, such that three copies of the ERR genes are now present in *S. cerevisiae*. *ERR1* and *ERR2* are contained in subtelomeric repeats that also contain the genes *PAU21* and *PAU22*, respectively. In fact, the gene order in each is conserved as *PAU21–ERR1–HSP33–FDH1* and *PAU22–ERR2–HSP32–FDH2*, respectively. It has been suggested that subtelomeric regions of chromosomes serve as a place for maintaining gene families that serve adaptive purposes (Fabre *et al*., 2005), and that enhanced rates of recombination and duplication within these regions lead to functional divergence that allows adaptation to new environments (Brown *et al*., 2010). If we accept the fact that subtelomeric regions have been evolving at a higher rate than the rest of the genome (Kellis *et al*., 2003), then the ERR genes have diverged from one another quite recently, or their sequence has been maintained for a specific role.

Pryde *et al*. (1995) first proposed that the conservation of ERR gene sequence suggests a selective pressure to maintain the function of the Err proteins. Fabre *et al*. (2005) have suggested that brewing or baking strains of yeast have specifically maintained gene families in subtelomeric regions of chromosomes because of positive selection. Again, this may suggest some roles for the ERR genes which have been lost in the closely related

DOI: 10.1002/yea

Saccharomyces sensu stricto yeast *S. bayanus* that was not subjected to the same environmental pressures (Pryde *et al*., 1995). Interestingly, although based on Southern hybridization data, Pryde *et al*. (1995) indicated a lack of ERR-like sequences in *S. paradoxus*, the yeast most closely related to *S. cerevisiae*, recent sequence data have revealed a single ERR-like gene in this yeast (Liti *et al*., 2009). What function, if any, these ERR genes carry out is still not clear. Wolfe and Shields (1997) note that the most striking physiological difference between *Saccharomyces* and other yeasts is its ability to ferment sugars vigorously under anaerobic conditions, producing ethanol, and we have shown here that the ERR gene products could function in glycolysis as part of the fermentative pathway.

Gene duplication and subsequent divergence is considered as one of the main forces behind the evolution of proteins with novel functions (Ohno, 1970). Of the four possible outcomes of gene duplication events described by Louis (2007), the one that seems most applicable here is that the two copies of the gene diverge such that they not only maintain the ability to complement each other but also take on non-overlapping functions, such as altered or expanded substrate specificity (Aharoni *et al*., 2005; Brown *et al*., 2010). This may be the case both between the *Saccharomyces cerevisiae* ENO genes and among the ENO and ERR genes. Both Eno1p and Eno2p can catalyse the glycolytic activity of enolase proteins, but Eno2p seems to be favoured for non-glycolytic functions of enolase, such as tRNA import into mitochondria (Entelis *et al*., 2006) and vacuole formation (Decker and Wickner, 2006). Here, we have shown that the ERR gene products also can carry out the glycolytic activity of enolases both *in vitro* and *in vivo*, although perhaps slightly less efficiently (based on both specific activities and growth on glucose), but we have not explored other possible functions of these proteins. If we look at the distribution of non-conserved residues in the Err proteins compared to the Eno proteins, we find the majority on the surface of the protein. These surface amino acids would be available to interact with other proteins. We know that enolase has functions in yeast not linked directly to glycolysis or gluconeogenesis that probably involve interactions with other proteins. These changes on the surface of the proteins may impair the ability of Err2 or Err3p to fulfil some of the other functions of Eno1p or Eno2p. On the other hand, they may contribute to some as-yet unknown functions of the ERR proteins. Dissecting the roles of individual ERR genes will require further experiments, including the construction of individual ERR null strains in the enolase double-null background.

Acknowledgements

This work was supported by a Discovery Grant (no. 121664) from the Natural Sciences and Engineering Research Council of Canada (to P.B.M.J.). We thank Dr Nina Entelis (CNRS-Université Louis Pasteur, Strasbourg) for providing strains and plasmids. We appreciate the critical reading of the manuscript and helpful suggestions of the anonymous reviewers.

Supporting information on the internet

The following supporting information may be found in the online version of this article:

Figure S1. The neighbour-joining and two equally parsimonious trees (length = 738) identified through phylogenetic analyses of amino acid sequences of enolase gene products of selected fungi

Table S1. Pairwise genetic distances or the number of amino acid differences, based on aligned amino acid sequences of enolase or enolase-like gene products in yeast

References

Aharoni A, Gaidukov L, Khersonsky O, *et al*. 2005. The 'evolvability' of promiscuous protein functions. *Nat Genet* **37**: 73–76.

Ausubel FM, Brent R, Kingston RE, *et al*. (eds). 1989. Current Protocols in Molecular Biology. Wiley: New York.

Boeke JD, LaCroute F, Fink GR. 1984. A positive selection for mutants lacking orotidine-5′-phosphate decarboxylase activity in yeast: 5-fluoro-orotic acid resistance. *Mol Gen Genet* **197**: 345–346.

Brachmann CB, Davies A, Cost GJ, *et al*. 1998. Designer deletion strains derived from *Saccharomyces cerevisiae* S288C: a useful set of strains and plasmids for PCR-mediated gene disruption and other applications. *Yeast* **14**: 115–132.

Brewer JM, Weber G. 1968. The reversible dissociation of yeast enolase. *Proc Natl Acad Sci USA* **59**: 216–223.

Brindle PK, Holland JP, Willett CE, *et al*. 1990. Multiple factors bind the upstream activation sites of the yeast enolase genes *ENO1* and *ENO2*: ABFI protein, like repressor activator protein RAP1, binds *cis*-acting sequences which modulate repression or activation of transcription. *Mol Cell Biol* **10**: 4872–4885.

Brown CA, Murray AW, Verstrepan KJ. 2010. Rapid expansion and functional divergence of subtelomeric gene families in yeast. *Curr Biol* **20**: 895–903.

DOI: 10.1002/yea

Chai G, Brewer JM, Lovelace LL, *et al*. 2004. Expression, purification and the 1.8 Å resolution crystal structure of human neuron-specific enolase. *J Mol Biol* **341**: 1015–1021.

Chen SH, Giblett ER. 1976. Enolase: human tissue distribution and evidence for three different loci. *Ann Hum Genet* **39**: 277–280.

Chin CCQ, Brewer JM, Wold F. 1981. The amino acid sequence of yeast enolase. *J Biol Chem* **256**: 1377–1384.

Choi ID, Jeong MY, Ham MS, *et al*. 2008. Novel Ree1 regulates the expression of *ENO1* via the Snf1 complex pathway in *Saccharomyces cerevisiae*. *Biochem Biophys Res Commun* **377**: 395–399.

Cohen R, Holland JP, Yokoi T, *et al*. 1986. Identification of a regulatory region that mediates glucose-dependent induction of the *Saccharomyces cerevisiae* enolase gene *ENO2*. *Mol Cell Biol* **6**: 2287–2297.

Cohen R, Yokoi T, Holland JP, *et al*. 1987. Transcription of the constitutively expressed yeast enolase gene *ENO1* is mediated by positive and negative *cis*-acting regulatory sequences. *Mol Cell Biol* **7**: 2753–2761.

Costanzo M, Baryshnikova A, Myers CL, *et al*. 2010. Charting the genetic interaction map of a cell. *Curr Opin Biotechnol* **22**: 66–74.

Costenoble R, Picotti P, Reiter L, *et al*. 2011. Comprehensive quantitative analysis of central carbon and amino-acid metabolism in *Saccharomyces cerevisiae* under multiple conditions by targeted proteomics. *Mol Syst Biol* **7**: 464–488.

Cuthbertson RA, Tomarev SI, Piatigorsky J. 1992. Taxon-specific recruitment of enzymes as major soluble proteins in the corneal epithelium of three mammals, chicken, and squid. *Proc Natl Acad Sci USA* **89**: 4004–4008.

Das S, Shevade S, LaCount DJ, *et al*. 2011. *Plasmodium falciparum* enolase complements yeast enolase functions and associates with the parasite food vacuole. *Mol Biochem Parasitol* **179**: 8–17.

da Silva Giotto MT, Hannaert V, Vertommen D, *et al*. 2003. The crystal structure of *Trypanosoma brucei* enolase: visualization of the inhibitory metal binding site III and potential as target for selective, irreversible inhibition. *J Mol Biol* **331**: 653–665.

Decker BL, Wickner WT. 2006. Enolase activates homotypic vacuole fusion and protein transport to the vacuole in yeast. *J Biol Chem* **281**: 14523–14528.

Deutscher D, Meilijson I, Kupiec M, *et al*. 2006. Multiple knockout analysis of genetic robustness in the yeast metabolic network. *Nat Genet* **38**: 993–998.

Dujon B, Sherman D, Fischer G, *et al*. 2004. Genome evolution in yeasts. *Nature* **430**: 35–44.

Duquerroy S, Camus C, Janin J. 1995. X-ray structure and catalytic mechanism of lobster enolase. *Biochemistry* **34**: 12513–12523.

Entelis N, Brandina I, Kamenski P, *et al*. 2006. A glycolytic enzyme, enolase, is recruited as a cofactor of tRNA targeting toward mitochondria in *Saccharomyces cerevisiae*. *Genes Dev* **20**: 1609–1620.

Fabre E, Muller H, Therizols P, *et al*. 2005. Comparative genomics in hemiascomycete yeasts: evolution of sex, silencing, and subtelomeres. *Mol Biol Evol* **22**: 856–873.

Faller LD, Baroudy BM, Johnson AM, *et al*. 1977. Magnesium ion requirements for yeast enolase activity. *Biochemistry* **16**: 3864–3869.

Fasolo J, Sboner A, Sun MG, *et al*. 2011. Diverse protein kinase interactions identified by protein microarrays reveal novel connections between cellular processes. *Genes Dev* **25**: 767–778.

Goffeau A, Barrell BG, Bussey H, *et al*. 1996. Life with 6000 genes. *Science* **274**: 546–567.

Hafner A, Obermajer N, Kos J. 2012. γ-Enolase C-terminal peptide promotes cell survival and neurite outgrowth by activation of the PI3K/Akt and MAPK/ERK signalling pathways. *Biochem J* **443**: 439–450.

Holland JP, Brindle PK, Holland MJ. 1990. Sequences within an upstream activation site in the yeast enolase gene *ENO2* modulate repression of *ENO2* expression in strains carrying a null mutation in the positive regulatory gene *GCR1*. *Mol Cell Biol* **10**: 4863–4871.

Huie MA, Scott EW, Drazinic CM. 1992. Characterization of the DNA-binding activity of GCR1: *in vivo* evidence for two GCR1-binding sites in the upstream activating sequence of TPI of *Saccharomyces cerevisiae*. *Mol Cell Biol* **12**: 2690–2700.

Ideker T, Thorsson V, Ranish JA, *et al*., 2001. Integrated genomic and proteomic analyses of a systematically perturbed metabolic network. *Science* **292**: 929–934.

Kang HJ, Jung S-K, Kim SJ, *et al*. 2008. Structure of human α-enolase (hENO1), a multifunctional glycolytic enzyme. *Acta Cryst* **D64**: 651–657.

Kathiresan T, Krishnan K, Krishnakumar V, *et al*. 2006. Triose phosphate isomerase, a novel enzyme-crystallin, and τ-crystallin in crocodile cornea. High accumulation of both proteins during late embryonic development. *FEBS J* **273**: 3370–3380.

Kellis M, Patterson N, Endrizzi M, *et al*. 2003. Sequencing and comparison of yeast species to identify genes and regulatory elements. *Nature* **423**: 241–254.

Kornblatt MJ. 2005. Changing the metal ion selectivity of rabbit muscle enolase by mutagenesis: effects of the G37A and G41A mutations. *Biochim Biophys Acta* **1748**: 20–25.

Kornblatt MJ, Kornblatt JA, Hancock MA. 2011. The interaction of canine plasminogen with *Streptococcus pyogenes* enolase: they bind to one another but what is the nature of the structures involved? *PLoS One* **6**: e28481.

Kűhnel K, Luisi BF. 2001. Crystal structure of the *Escherichia coli* RNA degradosome component enolase. *J Mol Biol* **313**: 583–592.

Lai LC, Kissinger MT, Burke PV, *et al*. 2008. Comparison of the transcriptomic 'stress response' evoked by antimycin A and oxygen deprivation in *Saccharomyces cerevisiae*. *BMC Genom* **9**: 627–640.

Larsen TM, Wedekind JE, Rayment I, *et al*. 1996. A carboxylate oxygen of the substrate bridges the magnesium ions at the active site of enolase: structure of the yeast enzyme complexed with the equilibrium mixture of 2-phosphoglycerate and phosphoenolpyruvate at 1.8 Å resolution. *Biochemistry* **35**: 4339–4358.

Lipson D, Raz T, Kieu A, *et al*. 2009. Quantification of the yeast transcriptome by single-molecule sequencing. *Nat Biotechnol* **27**: 652–658.

Liti G, Carter DM, Moses AM, *et al*., 2009. Population genomics of domestic and wild yeasts. *Nature* **458**: 337–341.

Liu H, Zhang Y, Yang W. 2000. How is the active site of enolase organized to catalyze two different reaction steps? *J Am Chem Soc* **122**: 6560–6570.

Louis EJ. 2007. Making the most of redundancy. *Nature* **449**: 673–674.

McAlister L, Holland MJ. 1982. Targeted deletion of a yeast enolase structural gene. *J Biol Chem* **257**: 7181–7188.

Mumberg D, Müller R, Funk M. 1995. Yeast vectors for the controlled expression of heterologous proteins in different genetic backgrounds. *Gene* **156**: 119–122.

Ni L, Bruce C, Hart C, *et al*. 2009. Dynamic and complex transcription factor binding during an inducible response in yeast. *Genes Dev* **23**: 1351–1363.

Ohno S. 1970. Evolution by Gene Duplication. Springer-Verlag: New York.

DOI: 10.1002/yea

Pal-Bhowmick I, Vora HK, Jarori GK. 2007. Subcellular localization and post-translational modifications of the *Plasmodium yoelii* enolase suggest moonlighting functions. *Malar J* **6**: 45–51.

Pearce JM, Edwards YH, Harris H. 1976. Human enolase isozymes: electrophoretic and biochemical evidence for three loci. *Ann Hum Genet* **39**: 263–276.

Poyner RR, Laughlin LT, Sowa GA, *et al*. 1996. Toward identification of acid/base catalysts in the active site of enolase: comparison of the properties of K345A, E168Q, and E211Q variants. *Biochemistry* **35**: 1692–1699.

Pryde FE, Huckle TC, Louis EJ. 1995. Sequence analysis of the right end of chromosome XV in *Saccharomyces cerevisiae*: an insight into the structural and functional significance of sub-telomeric repeat sequences. *Yeast* **11**: 371–382.

Ptacek J, Devgan G, Michaud G, *et al*. 2005. Global analysis of protein phosphorylation in yeast. *Nature* **438**: 679–684.

Renigunta A, Mutig K, Rottermann K, *et al*. 2011. The glycolytic enzymes glyceraldehyde 3-phosphate dehydrogenase and enolase interact with the renal epithelial K^+ channel ROMK2 and regulate its function. *Cell Physiol Biochem* **28**: 663–672.

Rider CC, Taylor CB. 1974. Enolase isoenzymes in rat tissues. Electrophoretic, chromatographic, immunological and kinetic properties. *Biochim Biophys Acta* **365**: 285–300.

Sharifpoor S, van Dyk D, Costanzo M, *et al*. 2012. Functional wiring of the yeast kinome revealed by global analysis of genetic network motifs. *Genome Res* **22**: 791–801.

Sherman F. 1991. Getting started with yeast. *Meth Enzymol* **194**: 3–21.

Sikorski RS, Heiter P. 1989. A system of shuttle vectors and yeast host strains designed for efficient manipulation of DNA in *Saccharomyces cerevisiae*. *Genetics* **122**: 19–27.

Sims PA, Reed GH. 2005. Method for the enzymatic synthesis of 2-phospho-D-glycerate from adenosine 5′-triphosphate and D-glycerate via D-glycerate-2-kinase. *J Mol Catal B: Enzym* **32**: 77–81.

Stec B, Lebioda L. 1990. Refined structure of yeast apo-enolase at 2.25 Å resolution. *J Mol Biol* **211**: 235–248.

Subramanian A, Miller DM. 2000. Structural analysis of α-enolase. Mapping the functional domains involved in down-regulation of the c-myc protooncogene. *J Biol Chem* **275**: 5958–5965.

Swofford DL. 2001. PAUP*: Phylogenetic Analysis Using Parsimony (*and other methods), v 4 [computer program]. Sinauer Associates: Sunderland, MA, USA.

Tarassov K, Messier V, Landry CR *et al*. 2008. An *in vivo* map of the yeast protein interactome. *Science* **320**: 1465–1470.

Thompson JD, Higgins DG, Gibson TJ. 1994. CLUSTALW — improving the sensitivity of progressive multiple sequence alignment through sequence weighting, position specific gap penalties and weight matrix choice. *Nucleic Acids Res* **22**: 4673–4680.

Torres EM, Sokolsky T, Tucker CM, *et al*. 2007. Effects of aneuploidy on cellular physiology and cell division in haploid yeast. *Science* **317**: 916–924.

Uemura H, Shiba T, Paterson M, *et al*. 1986. Identification of a sequence containing the positive regulatory region of *Saccharomyces cerevisiae* gene *ENO1*. *Gene* **45**: 67–75.

Uemura H, Shiba T, Machida M, *et al*. 1987. A positive regulatory sequence of the *Saccharomyces cerevisiae ENO1* gene. *J Biochem* **102**: 181–189.

Wedekind JE, Pyner RR, Reed GH, *et al*. 1994. Chelation of serine 39 to Mg^{2+} latches a gate at the active site of enolase: structure of the bis(Mg^{2+}) complex of yeast enolase and the intermediate analog phosphonoacetohydroxamate at 2.1 Å resolution. *Biochemistry* **33**: 9333–9342.

Wedekind JE, Reed GH, Rayment I. 1995. Octahedral coordination at the high-affinity metal site in enolase: crystallographic analysis of the Mg^{II}-enzyme complex from yeast at 1.9 Å resolution. *Biochemistry* **34**: 4325–4330.

Wellinger RJ, Zakian VA. 2012. Everything you ever wanted to know about *Saccharomyces cerevisiae* telomeres: beginning to end. *Genetics* **191**: 1073–1105.

Westhead EW, McLain G. 1964. A purification of brewers' and bakers' yeast enolase yielding a single active component. *J Biol Chem* **239**: 2464–2468.

Wistow GJ, Lietman T, Williams LA, *et al*. 1988. τ-Crystallin/α-enolase: one gene encodes both an enzyme and a lens structural protein. *J Cell Biol* **107**: 2729–2736.

Wolfe KH, Shields DC. 1997. Molecular evidence for an ancient duplication of the entire yeast genome. *Nature* **387**: 708–713.

Zhang E, Hatada M, Brewer JM, *et al*. 1994. Catalytic metal ion binding in enolase: the crystal structure of an enolase-Mn^{2+}-phosphonoacetohydroxamate complex at 2.4 Å resolution. *Biochemistry* **33**: 6295–6300.

Zhao S, Choy BSF, Kornblatt MJ. 2008. Effects of the G376E and G157D mutations on the stability of yeast enolase – a model for human muscle enolase deficiency. *FEBS J* **275**: 97–106.

DOI: 10.1002/yea